

Measuring anomalous Wtb couplings at e^-p collider

Sukanta Dutta^{a,1}, Ashok Goyal^{b,2}, Mukesh Kumar^{c,3}, Bruce Mellado^{d,4}

¹*SGTB Khalsa College, University of Delhi. Delhi-110007. India.*

²*Department of Physics and Astrophysics, University of Delhi. Delhi-110007. India.*

³*National Institute for Theoretical Physics, School of Physics, School of Physics and Mandelstam Institute for Theoretical Physics, University of the Witwatersrand, Johannesburg.*

⁴*University of the Witwatersrand, Private Bag 3, Wits 2050, Johannesburg, South Africa.*

Abstract We study the accuracy with which the lowest order CP conserving anomalous Wtb couplings in the single top quark production at the proposed large hadron electron collider (LHeC) can be probed. The one dimensional distribution of various kinematic observables at the parton level MC and their asymmetries arising due to the presence of anomalous couplings both in the hadronic and leptonic W decay is examined.

We find that at 95 % C.L. the anomalous coupling associated with the left handed vector current can be measured at an accuracy of the order of $\sim 10^{-2} - 10^{-3}$, while those associated with the right handed vector and left as well as right handed tensor currents have sensitivity at the order of $\sim 10^{-1} - 10^{-2}$ for the systematic uncertainty varying between 10%-1% at an integrated luminosity of 100 fb^{-1} . A comprehensive analysis of the combined covariance matrix derived from all one dimensional distributions of kinematical observables is used to compute the errors in anomalous couplings.

Keywords top, effective theory, anomalous couplings, Wtb

1 Introduction

The top quark provides an excellent opportunity for the study of electroweak symmetry breaking mechanism as well as to provide glimpse of new physics (NP) beyond the standard model (SM). The top quark decays almost exclusively in the $t \rightarrow bW^+$ channel.

The kinematic distributions of its decayed particles from top quark provide the information about the Wtb

vertex and associated new physics potentiality with the top quark production mechanism.

Within the SM, the Wtb vertex is purely left-handed, and its amplitude is given by the Cabibbo-Kobayashi-Maskawa (CKM) matrix element V_{tb} , related to weak interaction between a top and a b -quark and assuming $|V_{td}|^2 + |V_{ts}|^2 \ll |V_{tb}|^2$. The most general, lowest dimension, CP conserving, Lagrangian for the Wtb vertex is given by [1–3]

$$\begin{aligned} \mathcal{L}_{Wtb} = & \frac{g}{\sqrt{2}} \left[W_\mu \bar{t} \gamma^\mu (V_{tb} f_1^L P_L + f_1^R P_R) b \right. \\ & \left. - \frac{1}{2m_W} W_{\mu\nu} \bar{t} \sigma^{\mu\nu} (f_2^L P_L + f_2^R P_R) b \right] + h.c. \end{aligned} \quad (1)$$

where $f_1^L \equiv 1 + \Delta f_1^L$, $W_{\mu\nu} = \partial_\mu W_\nu - \partial_\nu W_\mu$, $P_{L,R} = \frac{1}{2}(1 \mp \gamma_5)$ are left- and right-handed projection operators, $\sigma^{\mu\nu} = i/2(\gamma^\mu \gamma^\nu - \gamma^\nu \gamma^\mu)$ and $g = e/\sin \theta_W$. In SM $|V_{tb}| f_1^L \simeq 1$, all other couplings f_2^L, f_1^R, f_2^R vanish at tree level. Their non-vanishing values are generated at the one loop level [4]. Wtb anomalous couplings f_i are constrained from flavor physics. The magnitudes of the right-handed vector and tensor couplings can be indirectly constrained from the measured branching ratio of the $b \rightarrow s\gamma$ process. Current 95% C.L. bounds based on

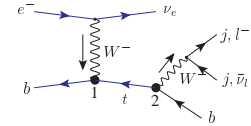


Fig. 1 Single anti-top quark production through charge current at the $e-p$ collider. The blobs at vertices 1 and 2 show the effective $W^- \bar{t}b$ couplings, which includes the SM contribution. Further W^- decays into hadronic mode via light quarks ($j \equiv \bar{u}, d, \bar{c}, s$) or leptonic mode ($l^- \equiv e^-, \mu^-$) with missing energy.

^ae-mail: sukanta.dutta@gmail.com

^be-mail: agoyal45@yahoo.com

^ce-mail: mukesh.kumar@cern.ch

^de-mail: bmellado@mail.cern.ch

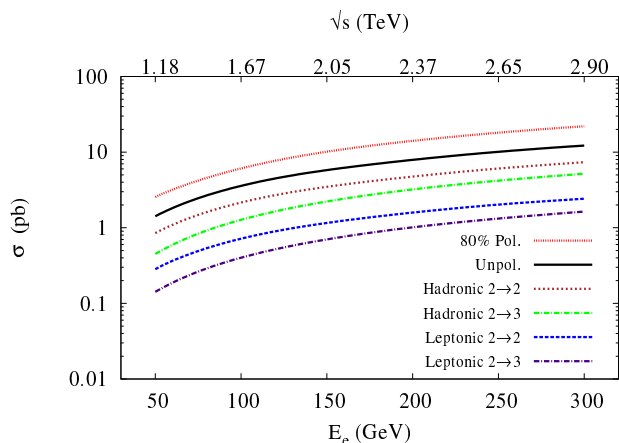


Fig. 2 Single anti-top quark production cross section at the LHeC with the variation of electron energy E_e and fixed proton energy $E_p = 7$ TeV. The top two curves depict the cross-section for $e^-p \rightarrow \nu_e \bar{t}$ from the 80 % polarized and unpolarized e^- beam, respectively. The third and the fifth curve corresponds to the branching of the unpolarized cross-section into hadronic and leptonic decay modes of W^- . The first and the third curve from the below corresponds to the cross-section for $e^-p \rightarrow \bar{t} \nu_e b$ branching to the leptonic and hadronic decay modes of W^- , respectively.

the CLEO data give $|f_1^R| \leq 4.0 \times 10^{-3}$ at the $2\text{-}\sigma$ level [5–7]. The branching ratio (BR) $\text{BR}(b \rightarrow s\gamma)$ is computed by neglecting $|f_i|^2$ terms in the matrix element squared and assuming only one anomalous coupling to be non-zero at a time. The upper and lower limits for $|V_{tb}| f_1^L$, f_1^R , f_2^L and f_2^R obtained from the B decays are $-0.13 \leq |V_{tb}| \Delta f_1^L \leq 0.03$, $-0.0007 \leq f_1^R \leq 0.0025$, $-0.0015 \leq f_2^L \leq 0.0004$ and $-0.15 \leq f_2^R \leq 0.57$, respectively [8]. If more than one coupling are taken non-zero simultaneously, their magnitudes in principle are not bound by $b \rightarrow s\gamma$ alone and the limits can be very different. Combining the analysis on $B_{d,s} = \bar{B}_{d,s}$ mixing and $B \rightarrow X_s l^+ l^-$, authors of reference [9] constrained Wtb couplings within an effective field theory framework.

The sensitivity of anomalous Wtb couplings can also be measured from W^\pm helicity distributions arising from top decays to their dominant Wb mode in the top pair production processes [10]. It can also be measured from the observed single top quark production cross section through W -boson exchange and has both the linear and quadratic terms in the effective couplings. Although the single top production in the SM is comparable to the $t\bar{t}$ pair production, it is quite challenging to make the extraction due to considerable backgrounds at the Tevatron [11, 12] and the LHC [13, 14]. $D\bar{O}$ with 5.4 fb^{-1} data reported a combined analysis of W boson helicity studies and the single top quark production cross section exclusively through Wtb vertex. This sets up-

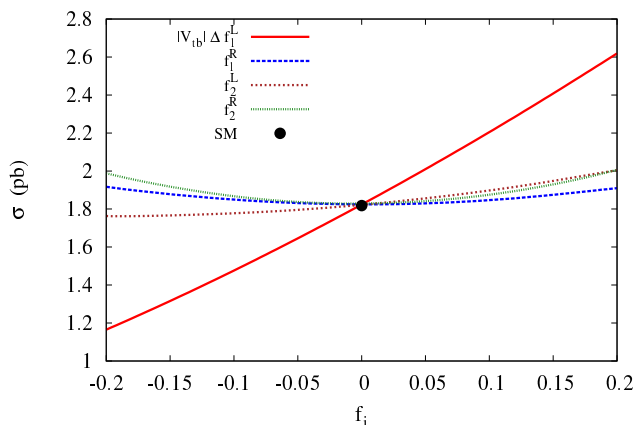


Fig. 3 Variation of the single anti-top quark production cross section with the effective Wtb couplings (taking one anomalous coupling at a time with SM) at the production and decay vertices, for fixed $E_p = 7$ TeV and $E_e = 60$ GeV.

per limits on anomalous Wtb couplings at 95 % C.L. viz. $|f_2^L| \leq 0.224$, $|f_1^R| \leq 0.548$, $|f_2^R| \leq 0.347$ (given in Table 1 of reference [15]). Sensitivity of the anomalous Wtb couplings on the cross-section of the associated tW production are also studied at LHC through γp collision at $\sqrt{s} = 14$ TeV for various luminosities and acceptance criterion [16]. The study of coefficients of dimension six operators affecting Wtb couplings from electroweak precision measurements [17, 18], suggest that the upper limits on these couplings are one order of magnitude weaker, to those obtained directly from the helicity fraction study of the top decay at NLO QCD [19].

The sensitivity of the effective couplings in (1) can be studied through one-dimensional distributions of kinematic observables. These distributions manifest a certain amount of associated asymmetry depending on the specific Lorentz structure, which can then be used as a discriminator to constraint these anomalous couplings. Based on associated asymmetries generated from the measured angular distributions of $\cos \theta^*$ defined in [20], the ATLAS collaboration [21] set limits on single anomalous couplings at 95% C.L. to be $-0.44 \leq \text{Re}(f_1^R) \leq 0.48$, $-0.24 \leq \text{Re}(f_2^L) \leq 0.21$ and $-0.49 \leq \text{Re}(f_2^R) \leq 0.15$. A combined constraint on anomalous couplings from CMS and ATLAS [22] shows the sensitivity of these couplings with respect to the helicity fraction in the top quark decays. Constraints on Wtb vertex based on the angular asymmetries constructed from ATLAS data and the t -channel single top cross section in CMS

⁰The cosine of the angle θ^* between the momentum direction of the charged lepton from the W -boson decay and the reversed momentum direction of the b quark from top-quark decay, both boosted into the W -boson rest frame.

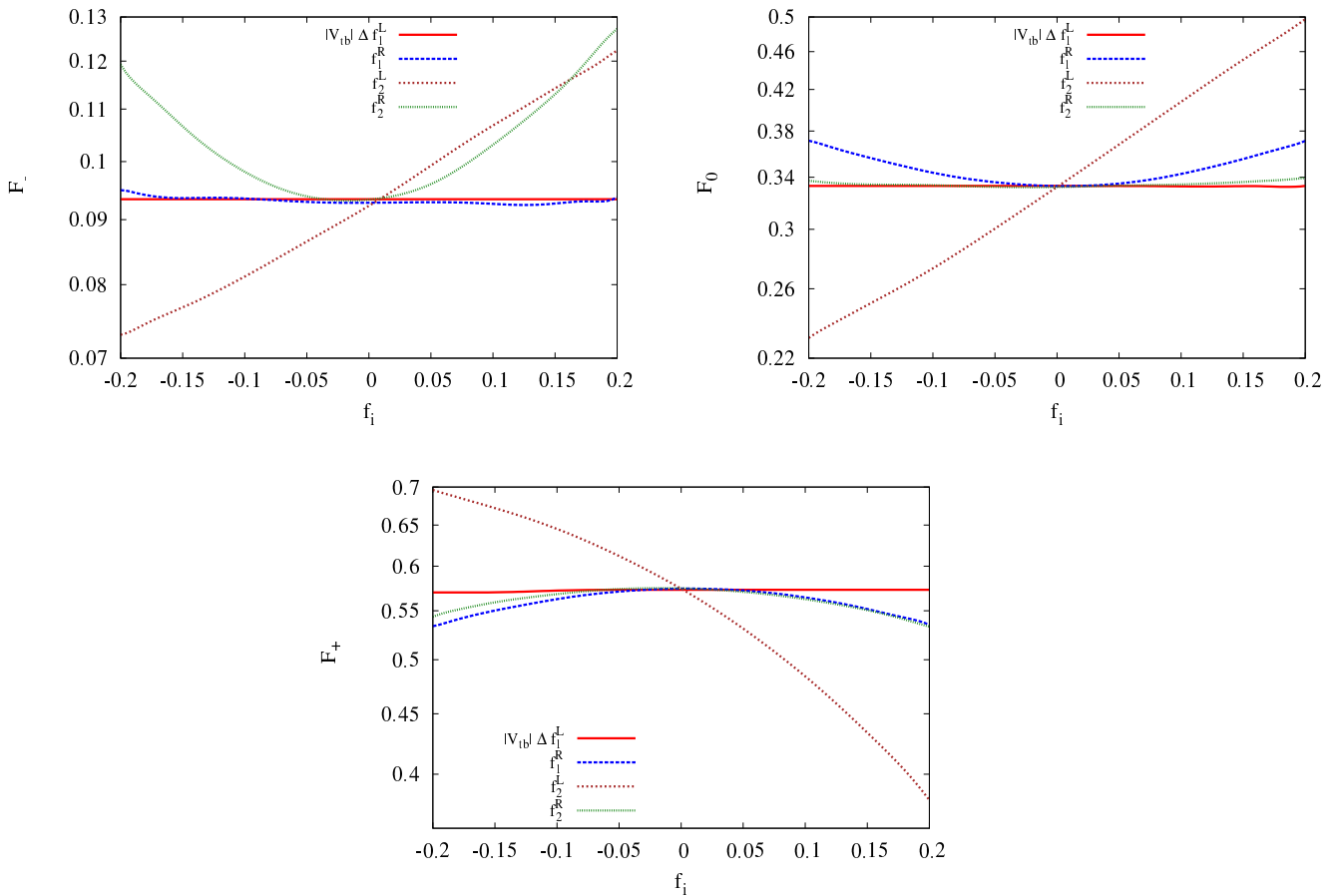


Fig. 4 The variation of helicity fractions \mathcal{F}_- , \mathcal{F}_0 and \mathcal{F}_+ as defined in the text with the anomalous coupling f_i .

have been analysed in [23]. A projected sensitivity of all anomalous top couplings have also been studied in reference [24].

Effects of anomalous coupling on angular distributions of the b -quark and μ^+ have been studied in e^+e^- linear collider with one specific semileptonic channel in the double resonance approximation for the t and \bar{t} production [25–28]. A preliminary study of the sensitivity of Wtb anomalous couplings on the single top quark production cross-section in e^-p collision for TESLA + HERA and LHC+CLIC energies has been performed in [29].

Recently a deep inelastic electron-nucleon scattering facility is proposed at the LHC, known as LHeC. It is proposed that an electron beam of 60 GeV will collide with 7 TeV proton beam simultaneous to the existing proton-proton collision experiments at the LHC [30–32]. The LHeC is expected to test the rich electroweak physics with precision. There has been some work on the physics goals of the collider [30–35]. The working group involved in the synergy between the LHC and the LHeC brought out an excellent report showing

the inter-dependencies of the physics reach and goals of both these colliders [36]. The LHeC is going to provide an unprecedented platform for studying the single top quark production as this has an advantage over the LHC and the Tevatron in terms of providing (a) a clean environment with suppressed background from strong interaction initiated processes, and (b) a kinematic reach for lepton-nucleon scattering at c.m. energy around 1.3 TeV [37–41].

Thus it is worthwhile to study the single top quark production and probe the Wtb anomalous couplings at the LHeC.

In Sec. 2 we analyse and study the single anti-top quark production and potential backgrounds, their yield, choice of selection cuts and kinematic distributions at the LHeC. We introduce kinematic asymmetries as estimators in Sec. 3, provide the exclusion contours based on bin analysis of distributions involving kinematic observables and finally using the method of optimal variables we give error correlation matrices and exclusion contours with 1% luminosity uncertainty. We discuss the impact of the luminosity uncertainty on the mea-

surement of the couplings and their correlations. The summary and analysis of our observations are given in Sec. 4.

2 Single anti-top quark production

In hadron colliders, the SM single top quark production at leading order is studied through three disparate non-interfering modes via s -, t - and Wt - channels, respectively and details can be found in [42]. The t - channel through charge current (CC) interactions dominates over all the other production mechanism. In the LHeC we can study the single top quark production only through t channel process $e^- \bar{b} \rightarrow \nu_e \bar{t} + X$ as shown in Figure 1. In sharp contrast to the LHC the absence of pile-up and underlying event effects at the LHeC, high rates of single anti-top production is expected to provide a better insight on Wtb anomalous couplings. The sensitivity of the Wtb couplings are also investigated through the sub-dominant associated tW production in references [43, 44].

We have implemented Wtb effective couplings corresponding to both chiral vector and tensor structures given by the Lagrangian (1) in MadGraph/MadEvent [45] using FeynRules [46]. The partonic cross sections are convoluted with CTEQ6L1 parton distribution functions (PDF) keeping factorization and renormalization scale $\mu_F = \mu_R = m_t = 172.5$ GeV. The mass of b -quark $m_b = 4.7$ GeV and W^\pm boson $m_W = 80.399$ GeV, assuming the SM value for $|V_{tb}| f_1^L = 1$.

The total top decay width which is one of the fundamental property of top physics is measured with precision from the partial decay width $\Gamma(t \rightarrow W b)$ in the t channel of the single top quark production. The effect of anomalous Wtb couplings in evaluating the decay width of the anti-top quark is consistently taken into account throughout our analysis for the signal cross-section.

Considering the five flavor constituents of proton we study the $2 \rightarrow 2$ process $e^- p \rightarrow \nu_e \bar{t} + X$ and probe the accuracy with which the anomalous couplings can be measured. The variation of the cross-section of the single top production in SM is studied with respect to the center of mass energy and electron energy in Figure 2 and we are in agreement with the earlier results given in [29]. We also show the effect of taking 80% beam polarization for electron, which results in the enhancement of the SM single top production cross section as the cross-section scales as $(1 + P_{e^-})$, P_{e^-} being the degree of polarization of the electron.

We also depict the varying contribution of $2 \rightarrow 3$ process $e^- p \rightarrow \bar{t} \nu_e b$ from the four flavor proton where the gluon splits into b, \bar{b} and \bar{b} participates in the interaction while b quark is produced in final state as

a spectator quark. This process is however suppressed in comparison to the $2 \rightarrow 2$ process $e^- p \rightarrow \bar{t} \nu_e$. This signal can be vetoed out by demanding the exclusion of two b jets. We do not consider this process for our analysis.

For the rest of the analysis we compute all cross-sections for the proposed LHeC with $E_{e^-} = 60$ GeV and $E_p = 7$ TeV as per recommendations given in the LHeC conceptual design report [30]. The total events are estimated with an integrated luminosity $L = 100$ fb $^{-1}$.

The new physics effect can arise either at the production vertex of the anti-top in the process $e^- p \rightarrow \bar{t} \nu_e \rightarrow \bar{b} W^- \nu_e$ or at the decay vertex. Figure 3 depicts the interplay of the interference terms for the left handed current and shows the variation of the cross section with respect to the variation in the anomalous couplings.

The stronger dependence of the cross section on the anomalous coupling Δf_1^L is because of the identical Lorentz structure associated with the SM and Δf_1^L and accordingly the constructive (destructive) interference becomes pronounced for positive (negative) $\Delta |f_1^L|$. Therefore the cross-section of left handed vector current mediated process varies as $[(1 + \Delta f_1^L) |V_{tb}|]^2$. On the other hand, the right handed current mediated processes vary as $|f_i^R|^2$ for $i = 1, 2$ and are therefore sub-dominant even in the presence of large $|f_i^R|$ because of the non-SM structure of the current.

We estimate and study the W^- helicity distributions arising from NP effects. The W polarization distribution distinguishes the contribution of anomalous couplings. We study the behaviour of the helicity fractions of the W^- in terms of ratios of the number of events $\mathcal{F}_- = N_-/N$, $\mathcal{F}_+ = N_+/N$ and $\mathcal{F}_0 = N_0/N$ where N_- , N_+ and N_0 are the left, right and longitudinally polarized W^- events and $N = N_+ + N_- + N_0$.

We vary the coupling and study its effect through the variation on these ratios in Figure 4. We observe that

- (a) The \mathcal{F}_- and \mathcal{F}_+ corresponding to the positive and negative polarized W^- 's show opposite trend with the variation of all effective couplings except $|v_{tb}| \Delta f_1^L$.
- (b) The helicity fractions \mathcal{F}_i associated with the left handed tensor current is most sensitive as it interferes with the SM and has a larger momentum dependence. Right handed vector chiral current shows an appreciable sensitivity *w.r.t.* \mathcal{F}_i helicity distribution.

The helicity fractions \mathcal{F}_- and \mathcal{F}_0 are also sensitive to the change in the coefficient of the right handed tensor current.

No.	Background Process	$p_{T,j,b} \geq 20$ GeV $ \eta_j \leq 5, \eta_b \leq 2.5$ $\Delta R_{j,b/j} \geq 0.4$ $\cancel{E}_T \geq 25$	$\Delta\Phi_{\cancel{E},j} \geq 0.4$ $\Delta\Phi_{\cancel{E},b} \geq 0.4$	$ m_{j_1j_2} - m_W \leq 22$ GeV	$\sigma_{\text{eff.}}$
1	$e^-p \rightarrow \nu_e W^- \bar{b}$ without anti-top line	7.5×10^{-3}	6.8×10^{-3}	4.5×10^{-3}	2.7×10^{-3}
2	$e^-p \rightarrow \nu_e jjj$	4.2×10^0	3.6×10^0	2.4×10^0	7.2×10^{-2}
3	$e^-p \rightarrow \nu_e cjj$ & $e^-p \rightarrow \nu_e \bar{c}jj$	1.5×10^0	1.2×10^0	8.6×10^{-1}	8.6×10^{-2}
4	$e^-p \rightarrow \nu_e c\bar{c}j$	5.8×10^{-2}	5.0×10^{-2}	3.2×10^{-2}	6.7×10^{-3}
5	$e^-p \rightarrow \nu_e b\bar{b}j$	2.5×10^{-2}	2.2×10^{-2}	5.6×10^{-3}	1.3×10^{-3}
6	$e^-p \rightarrow \bar{c}\nu_e$ ($\bar{c} \rightarrow W^- \bar{s}$)	2.5×10^{-2}	2.2×10^{-2}	1.5×10^{-2}	1.5×10^{-4}

Table 1 Cross-section of all background processes in pb for the hadronic channel with selection cuts. The effective background cross-section $\sigma_{\text{eff.}}$ is computed in the fifth column by multiplying b/\bar{b} tagging efficiency and/ or faking probability 1/10 and 1/100 corresponding to final state charm /anti-charm and light jets $j \equiv u, \bar{u}, d, \bar{d}, s, \bar{s}, g$, respectively.

Event Selection	$p_{T,j,b} \geq 20$ GeV $ \eta_j \leq 5, \eta_b \leq 2.5$ $\Delta R_{j,b/j} \geq 0.4$ $\cancel{E}_T \geq 25$	$\Delta\Phi_{\cancel{E},j} \geq 0.4$ $\Delta\Phi_{\cancel{E},b} \geq 0.4$	$ m_{j_1j_2} - m_W \leq 22$ GeV	Fiducial Efficiency	$S/\sqrt{S+B}$
SM	3.2×10^4	2.3×10^4	2.2×10^4	66.7 %	–
SM + $\sum_i \text{Bkg}_i$	6.5×10^4	5.0×10^4	4.0×10^4	61.5 %	–
$ V_{tb} \Delta f_1^L = .5$	7.3×10^4	5.0×10^4	5.0×10^4	68.0 %	1.92
$f_1^R = .5$	4.6×10^4	3.2×10^4	3.2×10^4	69.7 %	1.43
$f_2^L = .5$	4.9×10^4	3.6×10^4	3.6×10^4	73.2 %	1.55
$f_2^L = -.5$	3.4×10^4	2.3×10^4	2.3×10^4	69.6 %	1.40
$f_2^R = .5$	5.7×10^4	4.1×10^4	4.1×10^4	72.3 %	1.69

Table 2 Yield with selection cuts in the hadronic channel corresponding to the chosen anomalous coupling value of 0.5 at integrated luminosity $L = 100 \text{ fb}^{-1}$. The yield corresponding to $SM + \sum_i \text{Bkg}_i$ signify the total cumulative events of SM and all backgrounds after taking into account the b, \bar{b} faking/tagging efficiency. Yields corresponding to all anomalous couplings include the SM top background.

No.	Background Process	$p_{T,j,b,l} \geq 20$ GeV, $\Delta R_{j,b/j} \geq 0.4$, $\cancel{E}_T \geq 25$ $ \eta_j \leq 5, \eta_{b,l} \leq 2.5$	$\Delta\Phi_{\cancel{E},j} \geq 0.4$ $\Delta\Phi_{\cancel{E},b} \geq 0.4$ $\Delta\Phi_{\cancel{E},l} \geq 0.4$	$\sigma_{\text{eff.}}$
1	$e^-p \rightarrow l^- \bar{\nu}_l \nu_e j$		1.5×10^{-1}	1.4×10^{-3}
2	$e^-p \rightarrow l^- \bar{\nu}_l \nu_e c$ & $e^-p \rightarrow l^- \bar{\nu}_l \nu_e \bar{c}$		6.6×10^{-3}	6.1×10^{-4}
3	$e^-p \rightarrow l^- \bar{\nu}_l \nu_e b$ & $e^-p \rightarrow l^- \bar{\nu}_l \nu_e \bar{b}$ Without top line		3.6×10^{-3}	1.9×10^{-3}
4	$e^-p \rightarrow e^- l^- \bar{\nu}_l c$		1.5×10^{-2}	6.9×10^{-3}
5	$e^-p \rightarrow e^- l^- \bar{\nu}_l j$		1.2×10^{-1}	5.5×10^{-4}

Table 3 Cross-section of all background processes in pb for the leptonic channel with selection cuts. The effective background cross-section $\sigma_{\text{eff.}}$ is computed in the fourth column by multiplying b/\bar{b} tagging efficiency and/ or faking probability 1/10 and 1/100 corresponding to final state charm /anti-charm and light jets $j \equiv u, \bar{u}, d, \bar{d}, s, \bar{s}, g$, respectively. The background processes with two charged leptons are taken into consideration where one get lost in the beam pipe.

Event Selection	$p_{T,j,b} \geq 20$ GeV $ \eta_j \leq 5, \eta_b \leq 2.5$ $\Delta R_{j,b/j} \geq 0.4$ $\cancel{E}_T \geq 25$	$\Delta\Phi_{\cancel{E},j} \geq 0.4$ $\Delta\Phi_{\cancel{E},b} \geq 0.4$ $\Delta\Phi_{\cancel{E},l} \geq 0.4$	Fiducial Efficiency	$S/\sqrt{S+B}$
SM	1.2×10^4	1.1×10^4	92.0 %	–
SM + $\sum_i \text{Bkg}_i$	1.3×10^4	1.2×10^4	92.0 %	–
$ V_{tb} \Delta f_1^L = .5$	2.7×10^4	2.5×10^4	92.6 %	1.55
$f_1^R = .5$	1.7×10^4	1.6×10^4	94.1 %	1.23
$f_2^L = .5$	1.9×10^4	1.7×10^4	89.5 %	1.27
$f_2^L = -.5$	1.1×10^4	1.0×10^4	90.9 %	0.95
$f_2^R = .5$	2.2×10^4	2.0×10^4	90.9 %	1.38

Table 4 Yield with selection cuts in the leptonic channel corresponding to the chosen anomalous coupling value of 0.5 at integrated luminosity $L = 100 \text{ fb}^{-1}$. The yield corresponding to $SM + \sum_i \text{Bkg}_i$ signify the total cumulative events of SM and all backgrounds after taking into account the appropriate b, \bar{b} faking/tagging efficiency.

The helicity fractions are recently measured in the top quark pair events decaying leptonically and semi-leptonically with $\sqrt{s} = 8$ TeV at CMS detector in LHC with an integrated luminosity of 5 fb^{-1} [47]. Constraints obtained on F_- and F_0 are found to be consistent with SM but observations has left F_+ unconstrained.

Helicity fractions are studied through the reconstructed tops/ anti-tops in the experiment. Therefore sensitivity of these helicity fractions are subjected to systematic uncertainties arising from the re-construction algorithm efficiency and the determination of the angular distribution of all the decay products of the top/ anti-top. However one can overcome the above shortcomings with large statistics $e.g$ in LHC and improving the reconstruction of the most extreme bins in the angular distribution [48]. Moreover, it is better studied in hadron colliders where tops/ anti-tops are dominantly produced through strong interaction vertices for which the Wtb anomalous coupling would only depend on the decay vertices of tops/ anti-tops.

In this article, we proceed to extract more information on the sensitivity of anomalous couplings through one dimensional distribution of kinematic variables in the following section.

Finally we analyse the anti-top through the hadronic and leptonic decay modes of W 's. Henceforth, we have multiplied the cross-section (for processes having b or \bar{b} as its final state) with b, \bar{b} tagging efficiency $\epsilon_b = 0.6$.

2.1 Sensitivity in the Hadronic Mode

In order to study the sensitivity of the anomalous couplings introduced in equation (1), we examine the process $e^-p \rightarrow \bar{t}\nu_e, (\bar{t} \rightarrow W^-\bar{b}, W^- \rightarrow jj), j \equiv \bar{u}, d, \bar{c}, s$ at the LHeC and its potential backgrounds. We impose standard selection cuts as follows

- (i) Minimum transverse momentum for jets, \bar{b} -antiquark $p_{T_{b,j}} \geq 20$ GeV, $p_{T_{j,\bar{t}}} \geq 25$ GeV and minimum missing transverse energy $\cancel{E}_T \geq 25$ GeV.
- (ii) The pseudo-rapidity region for leptons and \bar{b} -antiquark processes mentioned in Table 1 is computed by taking $|\eta_{\bar{b},l}|$ is taken to be ≤ 2.5 , however for jets $|\eta_j| \leq 5$.
- (iii) Isolation cuts for lighter, heavy quarks and lepton require $\Delta R_{ij} \geq 0.4$ where $i, j \equiv$ leptons, jets and \bar{b} anti-quark.

In addition, we impose the following cuts to reduce the background

- (iv) The difference of azimuthal angle between missing energy \cancel{E}_T and jets, leptons, \bar{b} -antiquark should be $\Delta\phi \geq 0.4$.
- (v) To further reduce the background in the hadronic channel we reconstruct W^- from di-jets assuming

the jet energy resolution $\approx \frac{\sigma}{E} = \frac{0.6}{\sqrt{E}}$. In this setup the di-jet invariant mass resolution around the W^- mass is approximately 7%. Thus a mass window around 28% (4 times of this resolution at 2σ level) of the W mass ≈ 22 GeV is taken into consideration and hence di-jet invariant mass is allowed to satisfy $|m_{j_1 j_2} - m_W| \leq 22$ GeV.

The cross-section of the background processes and the effect of these selection cuts are given in the Table 1. The effective cross-section given in the fifth column is calculated after multiplying the $b\bar{b}$ tagging efficiency of 0.6. The b or \bar{b} faking probability is taken to be 1/100 for u, d, s quarks, antiquarks and 1/10 for c, \bar{c} quarks.

We observe that

- (a) The dominant background process is $e^-p \rightarrow \nu_e c / \bar{c} (jj)$ where $j \equiv u, \bar{u}, d, \bar{d}, s, \bar{s}, g$. The effective irreducible cross-section of the this background after imposing all cuts is ≈ 0.1 pb. The other dominant background is $e^-p \rightarrow \nu_e j j j$ which along with the first one constitute almost 94% of the total irreducible background 169 fb.
- (b) the cross-section of $e^-p \rightarrow \nu_e W^- \bar{b}$ is dominated by diagrams wherein the $W^- \bar{b}$ is generated from anti-top quarks. However, after multiplying with the appropriate branching ratio for the hadronic mode of W^- the cross-section is reduced to the order of 10^{-3} pb. We have also found that the potential background due to mis-tagging of one of the double b, \bar{b} events arising from the process to $e^-p \rightarrow \nu_e j \bar{b} \bar{b}$ is negligibly small.

To probe the effect of these cuts on the yield, we study all kinematic distributions in SM, other non-top backgrounds and compare them with contributions from new physics cases with the representative value of the effective coupling at 0.5. The analysis is summarized in Table 2 and the overall fiducial efficiencies of additional cuts are presented. The significance $S/\sqrt{S+B}$ give the sensitivity of the cross-section corresponding to these representative values. The yield of background processes mentioned in Table 1 is computed by taking the appropriate weight factor due to mis-tagging or tagging of light quarks and \bar{b} quark respectively.

The characteristics of the highest p_T jet j_1 , the final state \bar{b} and the missing transverse energy \cancel{E}_T are likely to bear the signature of the Wtb couplings at the production/ decay vertex. We reconstruct the W^- from jets at the final states to study the azimuthal angle separation between W^- and \bar{b} and missing energy \cancel{E}_T . We study one dimensional distributions of azimuthal angle (angle between the planes) $\Delta\phi_{\cancel{E}_T, j_1}, \Delta\phi_{\cancel{E}_T, \bar{b}}, \Delta\phi_{\cancel{E}_T, W}$ and $\Delta\phi_{\bar{b}, W}$ along with the $\cos\theta_{\bar{b}j_1}$ and $\Delta\eta_{\bar{b}j_1}$, where all angles are defined in the lab frame. Figure

5 exhibit these distributions. To study the distribution profile and shape variation, all histograms are normalized to unity to and are drawn for a anomalous coupling representative value 0.5. The normalized distributions corresponding to $|V_{tb}|\Delta f_1^L = \pm 0.5$ is identical to that of SM. However, on consideration of backgrounds the distribution profile of kinematical variable generated from $|V_{tb}|\Delta f_1^L = \pm 0.5$ shows distortion when compared to that of pure SM. The SM+ \sum Bkg_{*i*} distributions are drawn after summing the bin-wise contribution from each background process with appropriate factor as mentioned earlier.

In most of the distributions the new physics couplings play a significant role and clear distinction has been seen in profile with respect to combined effect SM and backgrounds. We observe from Figure 5 that the contribution of left and right handed tensorial Lorentz structures are distinguishable in most distributions. The distributions corresponding to (a) azimuthal angle between missing energy and highest p_T jet j_1 and (b) cosine of the angle between massive b quark and j_1 show a noticeable difference in the profile with respect to the right handed tensor chiral current.

2.2 Sensitivity in the Leptonic Mode

Similarly we study the yield of the leptonic decay mode of W^- through the process $e^-p \rightarrow \bar{\nu}_e, (\bar{t} \rightarrow W^- \bar{b}, W^- \rightarrow l^- \bar{\nu}_l), l^- \equiv e^-, \mu^-$ at the LHeC. We impose the standard selection cuts are same as those given in 2.1. The effects of these selection cuts are given in Table 3. The effective cross-section is given in the fourth column of this table. In general all background processes are sub-dominant. Reading this Table 3, we observe that

- (a) processes with a charged lepton, \cancel{E}_T and light jets, where the light jets can fake a b jet of the signal becomes negligibly small once they are screened through the selection cuts and multiplied by the appropriate faking probability factor.
- (b) background processes with two charged leptons where one of them vanishes in the beam pipe is negligible after the imposition of the selection cuts.

The fiducial efficiencies due to the additional cuts are computed for the representative value of couplings at ± 0.5 corresponding to the coefficient of the different chiral and Lorentz structures as given in (1). They are shown along with the significance in Table 4.

In the leptonic mode the final state charged lepton along with \bar{b} shows the characteristic features of the anomalous couplings. Further we study the sensitivity of the couplings through one dimensional distributions corresponding to azimuthal angle $\Delta\phi_{\cancel{E}_T, l_1}, \Delta\phi_{\cancel{E}_T, \bar{b}},$

along with the polar angle $\cos\theta_{\bar{b}l_1}$ and difference of pseudo-rapidity $\Delta\eta_{\bar{b}l_1}$ between \bar{b} and the charged lepton with highest p_T designated as l_1 . Figure 6 depict these distributions. As mentioned before all normalized distributions corresponding to $|V_{tb}|\Delta f_1^L = \pm 0.5$ are identical to that of SM single top production. We observe that f_2^L shows a distinguishable profile over others. However, the distribution $\Delta\phi_{\cancel{E}_T, l}$ is sensitive to all anomalous couplings.

3 Estimators and χ^2 analysis

3.1 Angular Asymmetries from Histograms

We construct the asymmetry from the distribution of kinematic observables in both the hadronic and leptonic modes. These asymmetries can be sensitive discriminators to distinguish the contribution from the different Lorentz structure due to their characteristic momentum dependence. We study the angular asymmetries with respect to the polar angle $\cos\theta_{ij}$, rapidity difference $\Delta\eta_{ij}$ and azimuthal angle difference $\Delta\phi_{ij}$, where i, j may be any partons (including \bar{b} -antiquark), charged lepton or missing energy. The associated asymmetries $A_{\theta_{ij}}, A_{\Delta\eta_{ij}}$ and $A_{\Delta\phi_{ij}}$ are defined as

$$A_{\theta_{ij}} = \frac{N_+^A(\cos\theta_{ij} > 0) - N_-^A(\cos\theta_{ij} < 0)}{N_+^A(\cos\theta_{ij} > 0) + N_-^A(\cos\theta_{ij} < 0)} \quad (2)$$

$$A_{\Delta\eta_{ij}} = \frac{N_+^A(\Delta\eta_{ij} > 0) - N_-^A(\Delta\eta_{ij} < 0)}{N_+^A(\Delta\eta_{ij} > 0) + N_-^A(\Delta\eta_{ij} < 0)} \quad (3)$$

$$A_{\Delta\phi_{ij}} = \frac{N_+^A(\Delta\phi_{ij} > \frac{\pi}{2}) - N_-^A(\Delta\phi_{ij} < \frac{\pi}{2})}{N_+^A(\Delta\phi_{ij} > \frac{\pi}{2}) + N_-^A(\Delta\phi_{ij} < \frac{\pi}{2})} \quad (4)$$

with $0 \leq \Delta\phi_{ij} \leq \pi$. The asymmetry A_α and its statistical error for N_+^A and N_-^A events where $N = (N_+^A + N_-^A) = L \cdot \sigma$ is calculated by using the following definition based on binomial distribution :

$$A_\alpha = a \pm \sigma_a, \quad \text{where } a = \frac{N_+^A - N_-^A}{N_+^A + N_-^A} \text{ and}$$

$$\sigma_a = \sqrt{\frac{1 - a^2}{L \cdot \sigma}}; \quad (\alpha = \cos\theta_{ij}, \Delta\eta_{ij}, \Delta\phi_{ij}) \quad (5)$$

Here $\sigma \equiv \sigma(e^-p \rightarrow \bar{\nu}_e, \bar{t} \rightarrow W^- \bar{b}) \times BR(W^- \rightarrow jj/l^- \bar{\nu}) \times \epsilon_b$ is the total cross-section in the respective channel after imposing selection cuts and $\epsilon_b = 0.6$ is the b/\bar{b} tagging efficiency.

Based on the one dimensional histograms given in Figures 5 and 6, we look for the asymmetry within a distribution generated due to the interplay of the SM, Background channels and a given anomalous coupling for two distinct hadronic and leptonic modes of W^- decay. Any large deviation from the combined asymmetry due to SM and background processes would then

imply that the associated kinematic observable is an optimal variable in determining the sensitivity of the given anomalous coupling. We provide these asymmetries constructed from the distributions in Table 5 and 6 for the hadronic and leptonic channels, respectively a representative value of the anomalous coupling 0.5. Any asymmetry with respect to distributions corresponding to $|V_{tb}|\Delta f_1^L$ is identical to the one in SM.

Asymmetries shown in Tables 5 and 6 are good estimators for preliminary studies. They give a handle for judging the ability of the measured observable to distinguish the contribution from an anomalous term in the Lagrangian. We observe in Table 5 that the couplings are sensitive in magnitude as well as sign of the asymmetry generated by $\cos\theta_{b_{j1}}$ distribution. But they may not be sensitive enough for the couplings which are one order of magnitude smaller than the representative value. In fact the whole distribution is essentially divided into two halves which correspond to only two bins with large bin-width.

3.2 Exclusion contours from bin analysis

In this subsection the sensitivity of couplings are obtained through χ^2 analysis, where we compute the sum of the variance of events over all bins. Thus more bin information is likely to yield better sensitivity than the asymmetries which are generated essentially by dividing the whole distribution into two equal bins.

To make the analysis more effective we switch on two effective anomalous couplings at a time with SM and all possible background processes with same final states. The χ^2 becomes a function of two effective anomalous couplings f_i, f_j and defined as

$$\chi^2(f_i, f_j) = \sum_{k=1}^N \left(\frac{\mathcal{N}_k^{\text{exp}} - \mathcal{N}_k^{\text{th}}(f_i, f_j)}{\delta\mathcal{N}_k^{\text{exp}}} \right)^2 \quad (6)$$

where $\mathcal{N}_k^{\text{th}}(f_i, f_j)$ and $\mathcal{N}_k^{\text{exp}}$ are the total number of events predicted by the theory involving f_i, f_j and measured in the experiment for the k^{th} bin. $\delta\mathcal{N}_k^{\text{exp}}$ is the combined statistical and systematic error δ_{sys} in measuring the events for the k^{th} bin. If all the coefficients f_i 's are small, then the experimental result in the k^{th} bin should be approximated by the SM and background prediction as

$$\mathcal{N}_k^{\text{exp}} \approx \mathcal{N}_k^{\text{SM}} + \sum_i \mathcal{N}_k^{\text{Bkg}_i} = \mathcal{N}_k^{\text{SM}+\sum_i \text{Bkg}_i}. \quad (7)$$

The error $\delta\mathcal{N}_k^{\text{SM}}$ can be defined as

$$\delta\mathcal{N}_k^{\text{SM}+\sum_i \text{Bkg}_i} = \sqrt{\mathcal{N}_k^{\text{SM}+\sum_i \text{Bkg}_i} \left(1 + \delta_{\text{sys}}^2 \mathcal{N}_k^{\text{SM}+\sum_i \text{Bkg}_i} \right)} \quad (8)$$

The χ^2 analysis due to un-correlated systematic uncertainties is studied for three representative values of δ_{sys} at 1%, 5% and 10 %, respectively.

The analysis is performed for both hadronic and leptonic observables which depend on the distributions shown in Figures 5 and 6. Using this definition of χ^2 in (6), we draw the exclusion contours on the six different two dimensional planes defined by the anomalous couplings $|V_{tb}|\Delta f_1^L, f_1^R, f_2^L$ and f_2^R . 68.3% and 95% C.L. Exclusion contours for the hadronic and leptonic channels are shown in Figures 7, 8 and 9, 10, respectively. For each pair of the couplings, the effect of the overall systematic uncertainty (includes luminosity measurement error etc.) is sketched for three representative values of $\delta_{\text{sys}} = 1\%, 5\%$ and 10% .

On examination of the exclusion contours in both decay modes we find that

- The sensitivity of measuring all anomalous couplings are affected by the systematic uncertainty δ_{sys} .
- The sensitivity of $|V_{tb}|\Delta f_1^L$ at 95% C.L. is of the $\sim 5 \times 10^{-3}$ and $\sim 3 \times 10^{-2}$ with systematic error of 1% and 10 %, respectively. The order of the sensitivity for other anomalous couplings varies as $\sim 10^{-2} - 10^{-1}$ at 95 % C.L. with the δ_{sys} varying between .01 to 0.1.

3.3 Errors and correlations

In order to constrain anomalous Wtb couplings further we adopt the method of optimal observables [49, 50] by using the full information from the distribution of kinematic observables. This technique of estimating the *equivalent maximum likelihood estimator* has been used in experimental analysis to compute the expected efficiencies in extracting the anomalous couplings from the experimental data [51–53]. In this method, all the anomalous couplings f_i , having different shape profiles from each other can be constrained simultaneously. For a given integrated Luminosity L , the statistical errors in the f_i and the correlations of the errors among anomalous coupling measurement can be obtained from the χ^2 which is a function of all anomalous couplings. Redefining the χ^2 of equation (6) in terms of the two anomalous couplings and the covariance matrix V we have

$$\chi^2(f_i, f_j) = \chi_{\text{min}}^2 + \sum_{i,j} (f_i - \bar{f}_i) [V^{-1}]_{ij} (f_j - \bar{f}_j) \quad (9)$$

A total of ten inverse covariant matrices V^{-1} can be generated from six and four distinct distributions of kinematic observables in hadronic and leptonic modes, respectively, using the approximation (7).

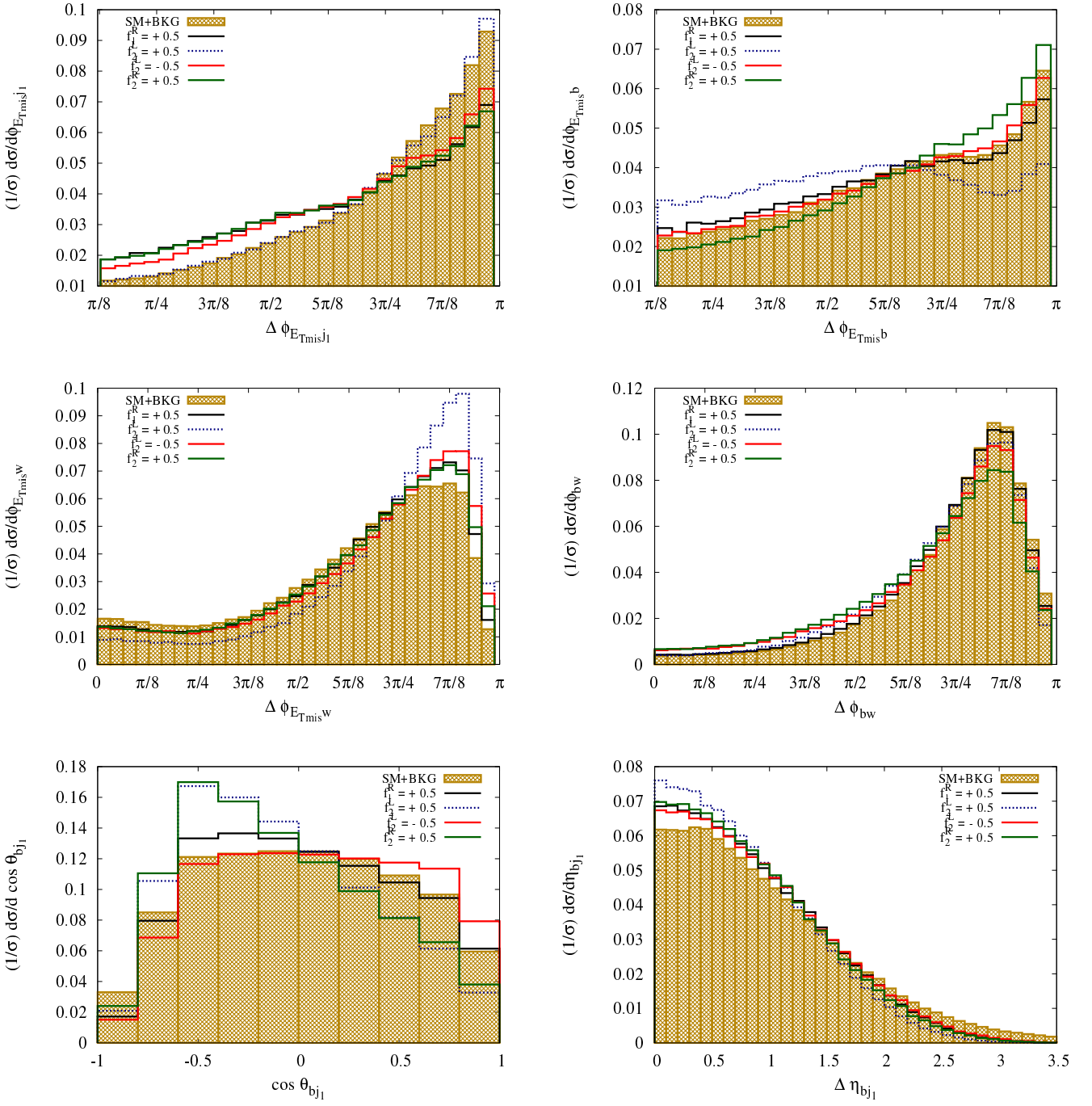


Fig. 5 Normalized distributions of $\Delta \phi_{E_T j_1}$, $\Delta \phi_{E_T \bar{b}}$, $\Delta \phi_{E_T W}$, $\Delta \phi_{bW}$, $\cos \theta_{\bar{b} j_1}$ and $\Delta \eta_{\bar{b} j_1}$ for hadronic decay mode of W^- , corresponding to SM and an anomalous coupling of 0.5. Here j_1 is the highest p_T jet. The normalized distributions corresponding to $|V_{tb}| \Delta f_1^L = \pm 0.5$ is identical to that of SM. All kinematic observables are measured in lab frame.

	$A_{\Delta\Phi_{\cancel{E}_T j_1}}$	$A_{\Delta\Phi_{\cancel{E}_T \bar{b}}}$	$A_{\Delta\Phi_{\cancel{E}_T W^-}}$	$A_{\Delta\Phi_{W^- \bar{b}}}$	$A_{\theta_{\bar{b} j_1}}$	$A_{\Delta\eta_{\bar{b} j_1}}$
SM + \sum_i Bkg _{<i>i</i>}	.532 ± .003	.282 ± .005	.503 ± .004	.799 ± .003	.023 ± .001	-.712 ± .003
$f_1^R = +.5$.327 ± .004	.231 ± .004	.564 ± .004	.778 ± .003	.0005 ± .004	-.806 ± .003
$f_2^L = -.5$.528 ± .004	.082 ± .004	.716 ± .003	.748 ± .003	-.196 ± .004	-.868 ± .002
$f_2^L = +.5$.390 ± .005	.269 ± .004	.585 ± .004	.683 ± .004	.106 ± .005	-.795 ± .003
$f_2^R = +.5$.330 ± .004	.363 ± .004	.566 ± .003	.656 ± .003	-.197 ± .004	-.823 ± .002

Table 5 Asymmetries and its error associated with the kinematic distributions in Figure 5 at an integrated luminosity $L = 100 \text{ fb}^{-1}$. These asymmetries are computed for a representative value of the anomalous coupling 0.5 along with SM.

	$A_{\Delta\Phi_{\cancel{E}_T l_1}}$	$A_{\Delta\Phi_{\cancel{E}_T \bar{b}}}$	$A_{\theta_{\bar{b} l_1}}$	$A_{\Delta\eta_{\bar{b} l_1}}$
SM + \sum_i Bkg _{<i>i</i>}	.384 ± .004	.710 ± .003	.551 ± .006	-.765 ± .007
$f_1^R = +.5$.484 ± .004	.702 ± .003	.332 ± .006	-.821 ± .003
$f_2^L = -.5$.526 ± .004	.620 ± .003	.410 ± .006	-.831 ± .002
$f_2^L = +.5$.353 ± .005	.812 ± .003	.392 ± .007	-.850 ± .003
$f_2^R = +.5$.424 ± .004	.684 ± .003	.507 ± .005	-.809 ± .003

Table 6 Asymmetries and its error associated with the kinematic distributions in Figure 6 at an integrated luminosity $L = 100 \text{ fb}^{-1}$. These asymmetries are computed for a representative value of the anomalous coupling 0.5 along with SM and all background processes.

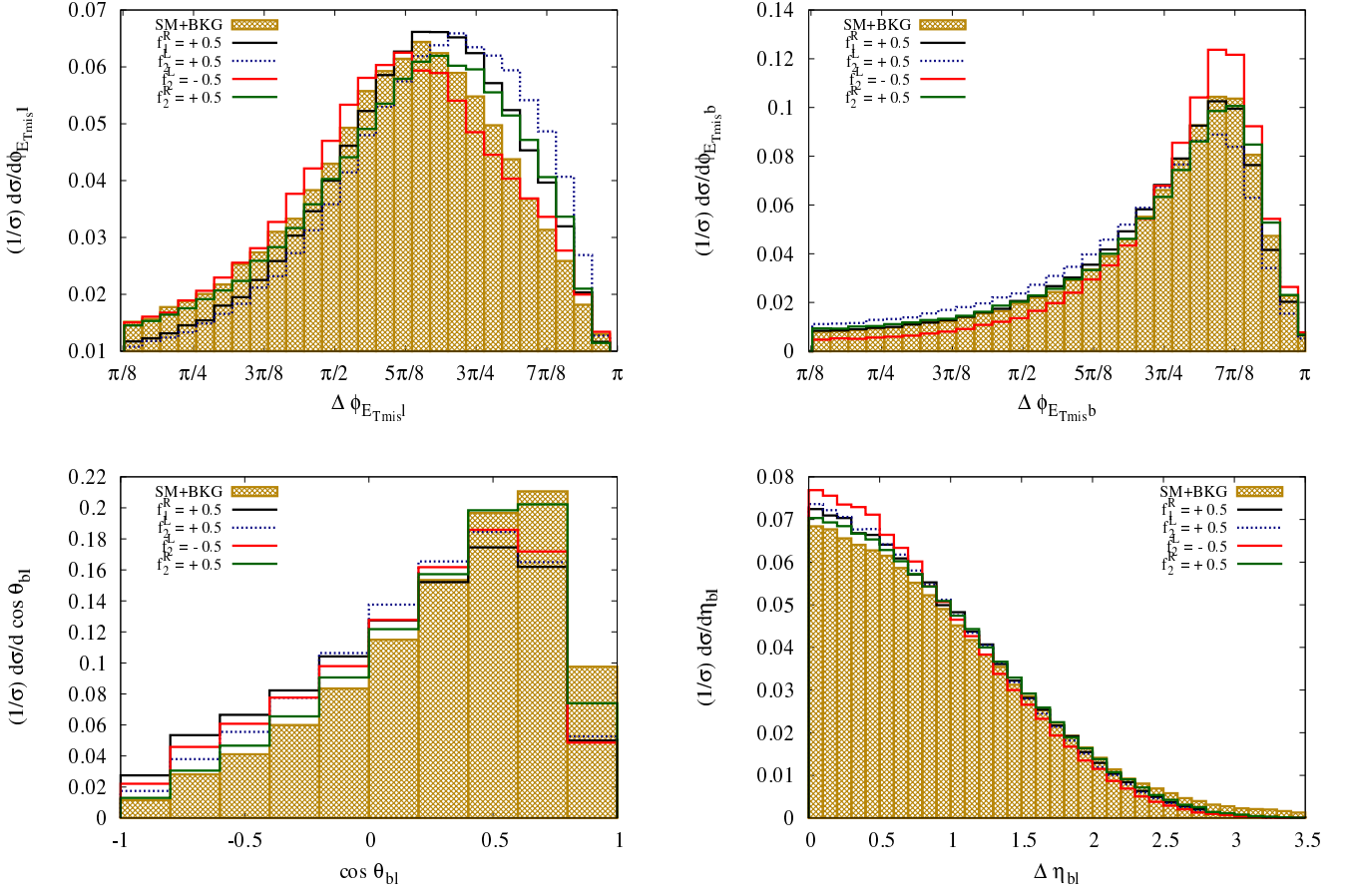


Fig. 6 Normalized distributions of $\Delta\phi_{E_{T}l_1}$, $\Delta\phi_{E_{T}\bar{b}}$, $\cos\theta_{\bar{b}l_1}$ and $\Delta\eta_{\bar{b}l_1}$ for leptonic decay mode of W^- corresponding to SM and an anomalous coupling of 0.5. Here l_1 is the highest p_T charged lepton. The normalized distributions corresponding to $|V_{tb}|\Delta f_1^L = \pm 0.5$ is identical to that of SM. All kinematic observables are measured in lab frame.

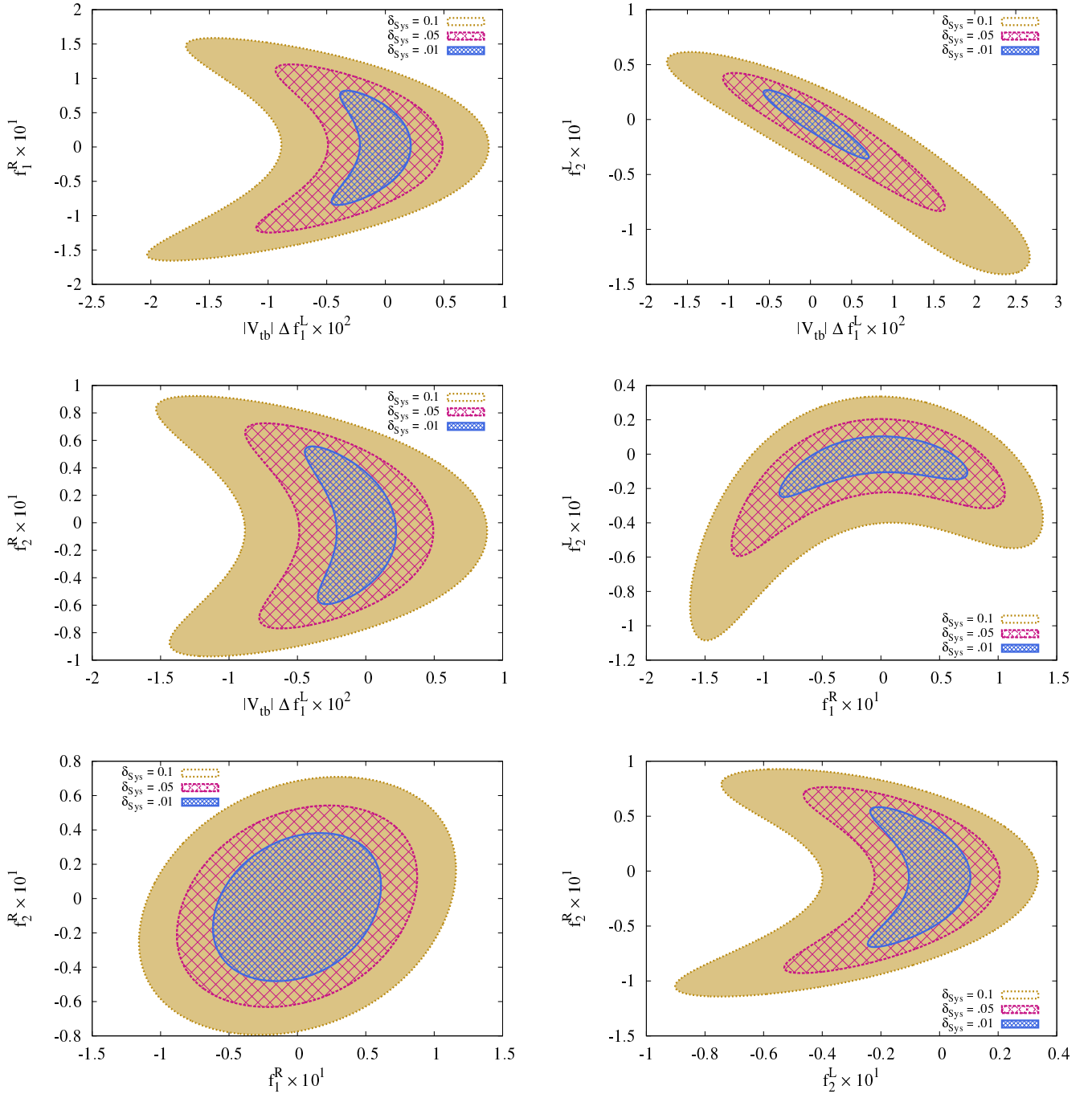


Fig. 7 68.3 % C.L. exclusion contours on the plane of $|V_{tb}| \Delta f_1^L - f_1^R$, $|V_{tb}| \Delta f_1^L - f_2^L$, $|V_{tb}| \Delta f_1^L - f_2^R$, $f_1^R - f_2^L$, $f_1^R - f_2^R$ and $f_2^L - f_2^R$ and based on combined bin analysis of all kinematic observables in the hadronic decay mode of W^- . A χ^2 analysis is performed by taking into account the deviation from SM and background process with the systematic error of 1%, 5% and 10%, respectively at an integrated luminosity of $L = 100 \text{ fb}^{-1}$.

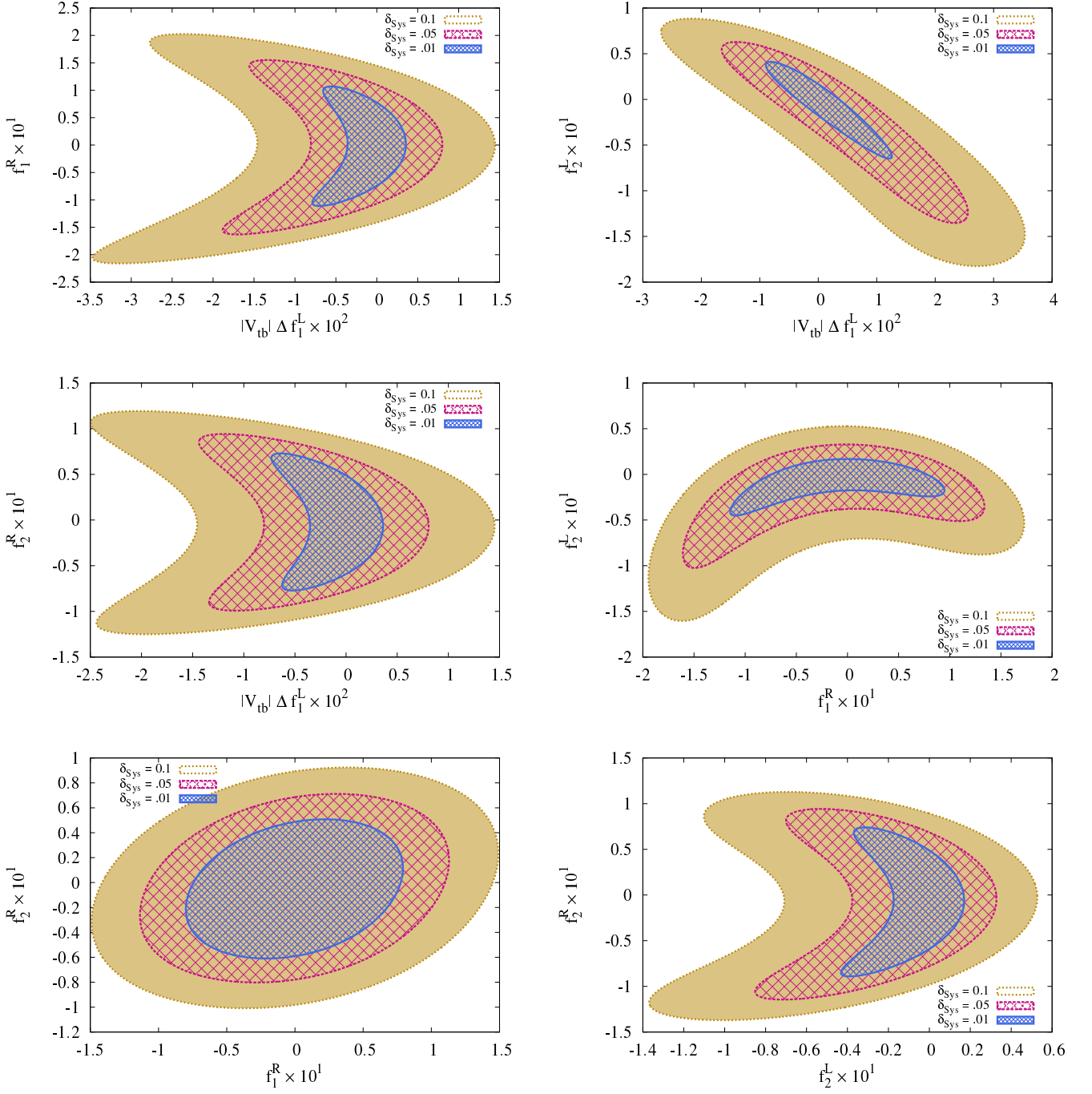


Fig. 8 95 % C.L. exclusion contours on the plane of $|V_{tb}| \Delta f_1^L - f_1^R$, $|V_{tb}| \Delta f_1^L - f_2^L$, $|V_{tb}| \Delta f_1^L - f_2^R$, $f_1^R - f_2^L$, $f_1^R - f_2^R$ and $f_2^L - f_2^R$ and based on combined bin analysis of all kinematic observables in the hadronic decay mode of W^- . A χ^2 analysis is performed by taking into account the deviation from SM and background process with the systematic error of 1%, 5% and 10%, respectively at an integrated luminosity of $L = 100 \text{ fb}^{-1}$.

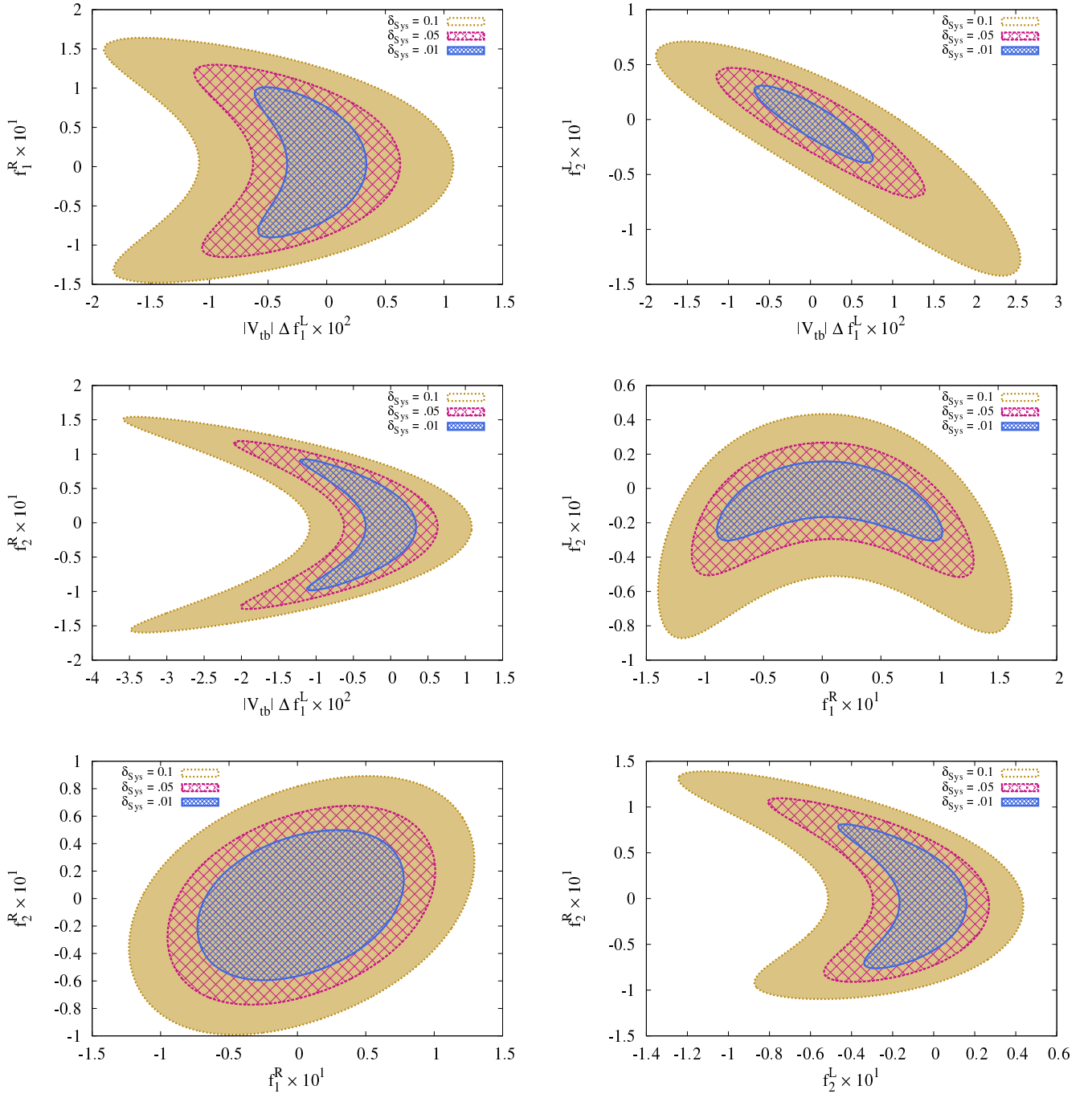


Fig. 9 68.3 % C.L. exclusion contours on the plane of $|V_{tb}| \Delta f_1^L - f_1^R$, $|V_{tb}| \Delta f_1^L - f_2^L$, $|V_{tb}| \Delta f_1^L - f_2^R$, $f_1^R - f_2^L$, $f_1^R - f_2^R$ and $f_2^L - f_2^R$ and based on combined bin analysis of all kinematic observables in the leptonic decay mode of W^- . A χ^2 analysis is performed by taking into account the deviation from SM and background process with the systematic error of 1%, 5% and 10%, respectively at an integrated luminosity of $L = 100 \text{ fb}^{-1}$.

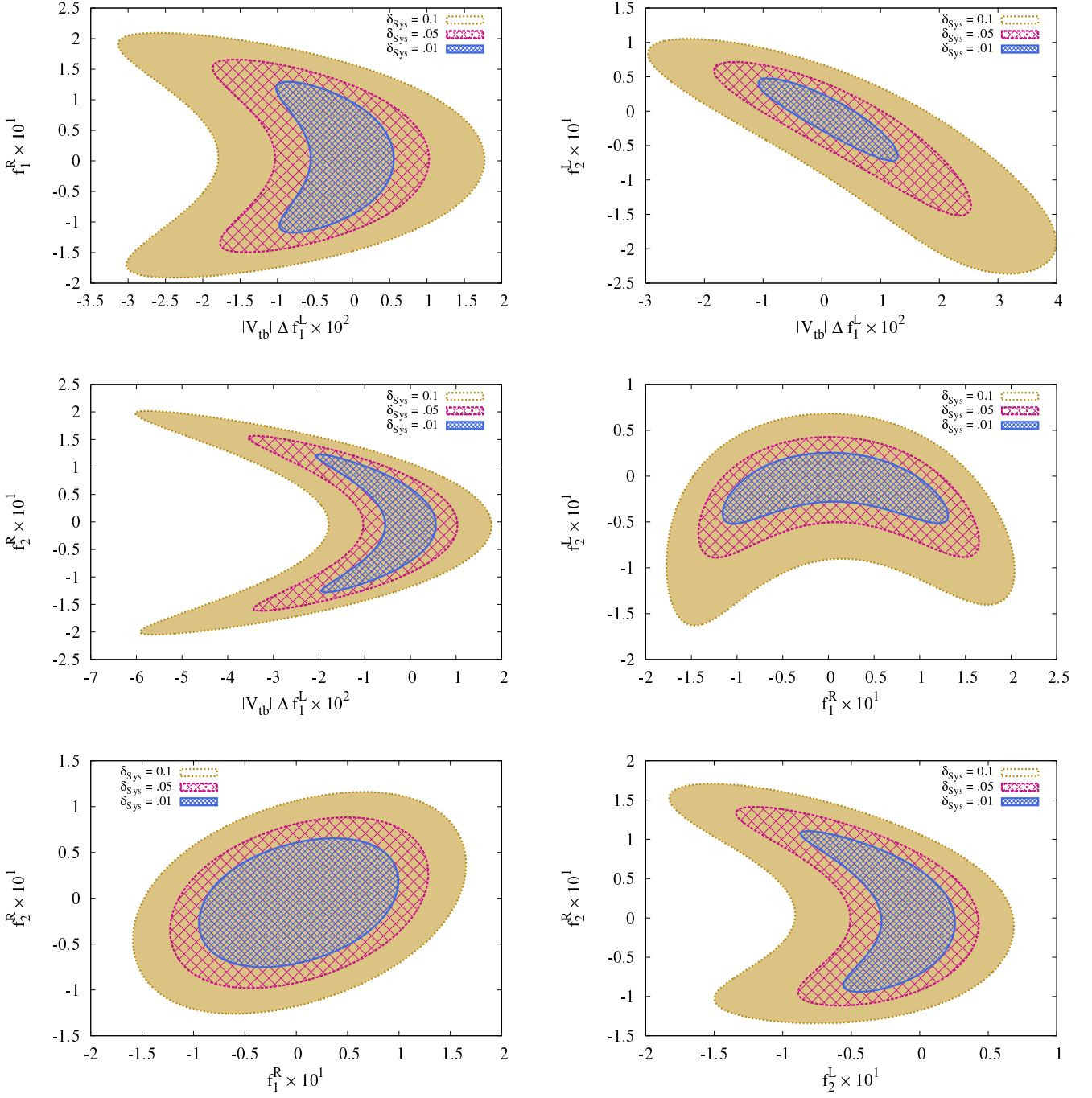


Fig. 10 95 % C.L. exclusion contours on the plane of $|V_{tb}| \Delta f_1^L - f_1^R$, $|V_{tb}| \Delta f_1^L - f_2^L$, $|V_{tb}| \Delta f_1^L - f_2^R$, $f_1^R - f_2^L$, $f_1^R - f_2^R$ and $f_2^L - f_2^R$ and based on combined bin analysis of all kinematic observables in the leptonic decay mode of W^- . A χ^2 analysis is performed by taking into account the deviation from SM and background process with the systematic error of 1%, 5% and 10%, respectively at an integrated luminosity of $L = 100 \text{ fb}^{-1}$.

If the SM prediction along with all dominant backgrounds gives a reasonably good description of the data in most of the phase space region, then the statistical errors Δf_i of f_i and their correlations are determined solely in terms of these six covariance matrices V as

$$f_i - \bar{f}_i = \pm \Delta f_i = \pm \sqrt{V_{ii}}, \quad \rho_{ij} = V_{ij} / \sqrt{V_{ii} V_{jj}}. \quad (10)$$

ρ_{ij} gives correlation coefficient between two distinct anomalous couplings f_i and f_j and gives the absolute error for a given anomalous coupling $f_i = f_j$. Δf_i gives the uncertainty with which these couplings will be measured at the LHeC. \bar{f}_i is the expected mean value in SM, which is zero for all anomalous couplings f_i .

Subsequently, an optimal analysis with an integrated luminosity $L = 100 \text{ fb}^{-1}$ is made after combining all kinematic observables in both hadronic and the leptonic modes, respectively.

The inverse of the covariance matrix V_{ij}^{-1} is generated from one dimensional histogram of each sensitive kinematic observable and the corresponding respective correlation matrix is computed. We combine all inverse covariant matrices to compute the combined χ^2 in the hadronic and leptonic modes separately.

The combined χ^2 reads as

$$\begin{aligned} & \chi_{\text{comb.}}^2(f_i, f_j) - \sum_{k=1}^n \chi_{\text{min}k}^2 \\ &= \sum_k \sum_{i,j} (f_i - \bar{f}_i) [V^{-1}]_{ij}^k (f_j - \bar{f}_j) \end{aligned} \quad (11)$$

Here $k \equiv$ number of distributions corresponding to the kinematic observables. $n = 6$ and 4 for hadronic and leptonic channels, respectively.

We thus provide the accuracy with which anomalous couplings can be measured from each of these distributions. The correlation matrices and the absolute errors in each and every couplings in the hadronic and leptonic modes are given below:

$$\begin{aligned} |V_{tb}| \Delta f_1^L &= \pm 4.5 \times 10^{-4} \begin{pmatrix} 1 \\ -0.07 & 1 \\ -0.04 & -0.07 & 1 \\ -0.03 & .006 & -0.02 & 1 \end{pmatrix}; \\ f_1^R &= \pm 7.2 \times 10^{-4} \\ f_2^L &= \pm 4.7 \times 10^{-4} \\ f_2^R &= \pm 3.2 \times 10^{-4} \end{aligned} \quad (a) \text{ hadronic mode} \quad (12)$$

$$\begin{aligned} |V_{tb}| \Delta f_1^L &= \pm 4.6 \times 10^{-4} \begin{pmatrix} 1 \\ -0.02 & 1 \\ -0.05 & -0.06 & 1 \\ -0.01 & .09 & -0.07 & 1 \end{pmatrix}; \\ f_1^R &= \pm 7.2 \times 10^{-4} \\ f_2^L &= \pm 8.3 \times 10^{-4} \\ f_2^R &= \pm 4.3 \times 10^{-4} \end{aligned} \quad (b) \text{ leptonic mode} \quad (13)$$

Up-till now we have considered the hadronic and leptonic modes of single anti-top production at the LHeC

to be two different probes for measuring these anomalous couplings. We now combine observations from both channels in terms of combined inverse covariance matrix. The global errors and correlations from the corresponding global combined covariance matrix is then given as

$$|V_{tb}| \Delta f_1^L = \pm 3.2 \times 10^{-4} \begin{pmatrix} 1 \\ -0.05 & 1 \\ -0.04 & -0.06 & 1 \\ -0.02 & .03 & -0.04 & 1 \end{pmatrix}; \quad (14)$$

$$\begin{aligned} f_1^R &= \pm 4.6 \times 10^{-4} \\ f_2^L &= \pm 4.2 \times 10^{-4} \\ f_2^R &= \pm 2.6 \times 10^{-4} \end{aligned}$$

It is worthwhile to mention that we have not yet considered any systematic error in the covariance analysis. On comparing the errors given in equations (13a) and (13b) corresponding to hadronic and leptonic modes, respectively and errors for the global combined analysis in equation (14) with those in section 3.2, we find that the sensitivity of $|V_{tb}| \Delta f_1^L$ and others are found to have increased by one and two orders of magnitude, respectively.

We have computed all the errors and their correlations based on 60 % b tagging efficiency ϵ_b along with 10% and 1% b faking probability by charm and light jets respectively. One can however, take these parameters in the χ^2 analysis explicitly rather than as an overall multiplying factor in the respective cross-sections. Since, we consider processes with same final states (same number of b, \bar{b}) for the signal as well as the dominant SM top background, the optimal analysis shows that the sensitivity of the errors in the measurement of these couplings will scale as $1/\sqrt{\epsilon_b}$ for a given luminosity and χ^2 .

Assuming the measured luminosity to be the true luminosity, the accuracy with which the anomalous couplings are measured scales as $1/\sqrt{L}$.

3.3.1 Luminosity Error

An error in the measurement of luminosity is however, is likely to affect the measurements of some effective couplings. It is thus instructive to study the impact of uncertainty in luminosity measurement on the sensitivity of anomalous Wtb couplings. The true luminosity L can be estimated as

$$L \equiv \beta \bar{L}, \beta = 1 \pm \Delta\beta, \quad (15)$$

where \bar{L} is the measured mean value, and $\Delta\beta$ is its one σ uncertainty. With the inclusion of the luminosity uncertainty the $\chi_{\text{comb.}}^2$ definition given in (9) is modified to

$$\begin{aligned} & \chi_{\text{comb.}}^2(f_i, f_j) \rightarrow \chi_{\text{comb.}}^2(f_i, f_j, \beta) \equiv \\ & \sum_{k=1}^m \sum_{i=0}^n \sum_{j=0}^n (f_i - \bar{f}_i) [V^{-1}]_{ij}^k (f_j - \bar{f}_j) + \left(\frac{\beta_k - 1}{\Delta\beta_k} \right)^2 \end{aligned} \quad (16)$$

Here $[V^{-1}]_{ij}^k$ is now $(n+1) \times (n+1)$ matrix with $f_0 = \beta - 1$. The luminosity uncertainty $\Delta\beta_k \equiv \Delta\beta$ is same for all kinematic observables at a given collision energy. Here $n \equiv 0, 1, 2, 3, 4$ corresponding to luminosity factor β and four anomalous couplings. $m = 6$ (4) corresponds to the number of kinematic observables for hardonic (leptonic) mode.

It is straightforward to integrate out the $f_0 = 1 - \beta$ dependence and obtain the probability distribution of the parameters f_1 to f_n in the presence of the luminosity uncertainty. $|V_{tb}| \Delta f_1^L$ is the only coupling whose weight function is identical to the SM distribution at tree level. The other effective couplings get the SM contribution at the one-loop level and it is thus likely that the statistical errors dominate over systematics. Therefore errors coming from the luminosity uncertainty can then be safely neglected for the other three couplings namely f_1^R , f_2^L and f_2^R .

The impact of the luminosity uncertainty can thus be accounted algebraically by using the χ^2 functions written in term of Δf_1^L . Redefining our $\chi_{\text{comb.}}^2$ function as

$$\begin{aligned} \chi_{\text{comb.}}^2(f_i, f_j, \beta) = \\ \chi_{\text{comb.}}^2 \left(\Delta f_1^L \rightarrow \Delta f_1^{L'} = \Delta f_1^L + \frac{\beta - 1}{2} \right) + \left(\frac{\beta - 1}{\Delta\beta} \right)^2 \\ = \sum_{k=1}^m \sum_{i=0}^n \sum_{j=0}^n f'_i [V^{-1}]_{ij}^k f'_j + \left(\frac{\beta_k - 1}{\Delta\beta_k} \right)^2 \end{aligned} \quad (17)$$

where $\Delta f_1^{L'} = \Delta f_1^L + (\beta - 1)/2$ and $f'_i \equiv f_i$ (for $i \neq 1$) The luminosity uncertainty in the $\chi_{\text{comb.}}^2$ function in equation (17) can be factored out as

$$\begin{aligned} \chi_{\text{comb.}}^2 = \left[\frac{\beta - 1}{\Delta\beta^{\text{eff}}} + \Delta\beta^{\text{eff}} R \right]^2 + \tilde{\chi}_{\text{comb.}}^2, \quad \text{where} \\ \{\Delta\beta^{\text{eff}}\}^{-2} = \frac{1}{\Delta\beta^2} + \frac{1}{4} [V^{-1}]_{11}; R = \frac{1}{2} \sum_{a=1}^4 f_a [V^{-1}]_{1a}; \end{aligned} \quad (18)$$

The new $\tilde{\chi}_{\text{comb.}}^2$ is the reduced combined χ^2 function, which can be re-written as

$$\tilde{\chi}_{\text{comb.}}^2 = \chi_{\text{comb.}}^2 - (\Delta\beta^{\text{eff}})^2 R^2 \quad (19)$$

The reduced χ^2 function can now be used to study the constraints on the effective couplings in the presence of the luminosity uncertainty. It is worth mentioning that correlations between the $|V_{tb}| \Delta f_1^L$ with other couplings are affected due to the presence of the second term in equation (19).

Following the optimal analysis by incorporating the luminosity uncertainty and the reduced $\tilde{\chi}_{\text{comb.}}^2$, we get 4×4 covariance matrix. The modified correlation matrices based on the combined study of the six and four

kinematical distributions from hadronic and leptonic modes, respectively at an integrated luminosity of $L = 100 \text{ fb}^{-1}$ can now be computed for different luminosity uncertainty factor β . We give a spectrum of three correlation matrices corresponding to the three choices for $\Delta\beta =$ at 1%, 5% and 10%, respectively:

$$\begin{aligned} |V_{tb}| \Delta f_1^L = \pm 5.0 \times 10^{-3} \begin{pmatrix} 1 & & & \\ f_1^R = \pm 4.7 \times 10^{-4} & -0.003 & 1 & \\ f_2^L = \pm 4.2 \times 10^{-4} & -0.003 & -0.068 & 1 \\ f_2^R = \pm 2.6 \times 10^{-4} & -0.002 & .032 & -0.041 & 1 \end{pmatrix}; \\ \text{(a) } \Delta\beta = 1\% \end{aligned} \quad (20)$$

$$\begin{aligned} |V_{tb}| \Delta f_1^L = \pm 2.5 \times 10^{-2} \begin{pmatrix} 1 & & & \\ f_1^R = \pm 4.6 \times 10^{-4} & 0 & 1 & \\ f_2^L = \pm 4.2 \times 10^{-4} & 0 & -0.068 & 1 \\ f_2^R = \pm 2.6 \times 10^{-4} & 0 & .032 & -0.041 & 1 \end{pmatrix}; \\ \text{(b) } \Delta\beta = 5\% \end{aligned} \quad (21)$$

$$\begin{aligned} |V_{tb}| \Delta f_1^L = \pm 5.0 \times 10^{-2} \begin{pmatrix} 1 & & & \\ f_1^R = \pm 4.6 \times 10^{-4} & 0 & 1 & \\ f_2^L = \pm 4.2 \times 10^{-4} & 0 & -0.068 & 1 \\ f_2^R = \pm 2.6 \times 10^{-4} & 0 & .032 & -0.041 & 1 \end{pmatrix}; \\ \text{(c) } \Delta\beta = 10\% \end{aligned} \quad (22)$$

It is observed from equations (20), (21) and (22) that the sensitivity of all couplings except $|V_{tb}| \Delta f_1^L$ remain same as before given in (14). The sensitivity of $|V_{tb}| \Delta f_1^L$ which has same weight function as SM is however, reduced by one order of magnitude $\sim 10^{-3}$ corresponding to luminosity uncertainty 1%. The error in $|V_{tb}| \Delta f_1^L$ is now comparable to that obtained in the bin analysis with 1% systematic error. Following the same suite of bin analysis the sensitivity further worsens by an order of magnitude $\sim 10^{-2}$ with increased luminosity uncertainty at 5% -10% uncertainty.

On assumption that the statistical error might dominate over the systematics in the determination of all other couplings, we observe that they are not affected due to the varying $\Delta\beta$ as mentioned in the definition of $\chi_{\text{comb.}}^2$. This is in sharp contrast to that observed in bin analysis where all couplings are affected by the systematic uncertainty.

The correlations of f_1^R , f_2^L and f_2^R with $|V_{tb}| \Delta f_1^L$ are drastically reduced for $\Delta\beta = .01$ and finally becomes vanishingly small for $\Delta\beta = .05$ and $\Delta\beta = 0.10$. However, the correlations among f_1^R , f_2^L and f_2^R remain same as given in equation (14).

As an illustration, we study the variation in total error measurement of $|V_{tb}| \Delta f_1^L$ based on this optimal analysis with a fixed luminosity uncertainty $\Delta\beta$. In Figure 11, the variation of the total error in the estimation of $|V_{tb}| \Delta f_1^L$, with the luminosity for a given $\Delta\beta$ is

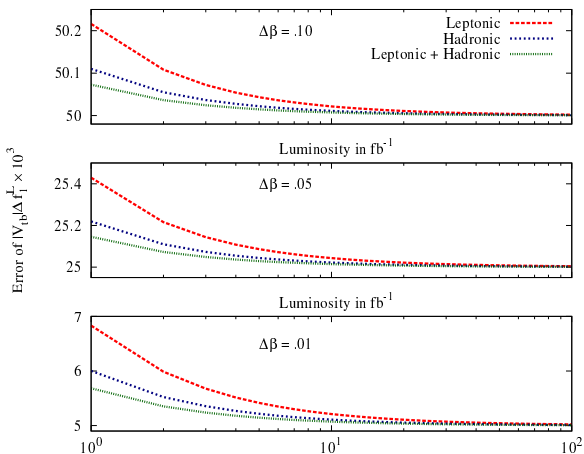


Fig. 11 Variation of the total error of $|V_{tb}| \Delta f_1^L$ with the luminosity for a given luminosity uncertainty of 1%, 5% and 10%, corresponding to the kinematical distributions from hadronic, leptonic and combined decay modes of W^- , respectively.

shown. Thus the error in the anomalous coupling not only depends on the high magnitude of the luminosity, but also on its measured value.

4 Observations and Discussion

An attempt has been made to study and investigate the sensitivity of the measurement of anomalous Wtb couplings associated with the left or right vector and tensor chiral currents. The LHeC being comparatively clean with respect to pp and $p\bar{p}$ colliders, provides an excellent environment to study the electroweak production of single anti-top. We analyse the effect of anomalous couplings in the Wtb vertex by examining its one dimensional distributions.

4.1 Observations

We summarize our results as follows :

- (i) It is found that asymmetries of kinematic variables constructed from respective one dimensional distributions can discriminate the effect of non-SM contribution through new vector and tensor chiral currents except for $|V_{tb}| \Delta f_1^L$, as shown in Tables 5 and 6, for anomalous couplings are of the order of $\sim 10^{-1}$. The asymmetry study suggests that the distribution of the cosine of angle between the tagged \bar{b} quark and the highest p_T jet j_1 in the hadronic decay mode of W^- to be the most sensitive observable.
- (ii) We have conducted a χ^2 analysis based on the differential events of all kinematic variables for hadronic

and leptonic modes in SM and background channels. This gives the exclusion contours on the anomalous couplings plane. Contours at 68 % and 95 % are provided for both hadronic and leptonic decay modes of W^- in Figures 7 and 9 and in Figures 8 and 10 respectively.

The sensitivity of $|V_{tb}| \Delta f_1^L$ at 95% C.L. is found to be of the order of $\sim 10^{-3} - 10^{-2}$ with the corresponding variation of 1% - 10% in the systematic error (which includes the luminosity error). The order of the sensitivity for other anomalous couplings varies between $\sim 10^{-2} - 10^{-1}$ at 95 % C.L.

We find that the sensitivity of the anomalous couplings can be increased with the increase in the luminosity as the couplings scales as $1/\sqrt{L}$ for a given χ^2 . Thus for 1 ab^{-1} the sensitivity of all f_i 's are going to be roughly improved by a factor of ≈ 0.31 . Similarly, for a given integrated true luminosity and χ^2 , an n fold increase in b -tagging efficiency would increase the sensitivity of the anomalous couplings by $1/\sqrt{n}$.

- (iii) Adopting the technique of the optimal observable, we obtained the global combined error sensitivity of all couplings is of the order of $\sim 10^{-4}$ in the absence of any systematic uncertainty.
- (iv) Lastly, we have extended our optimal analysis to include the luminosity uncertainty factor in addition to four anomalous couplings. The increasing luminosity error reduces the sensitivity of $|V_{tb}| \Delta f_1^L$ and its correlation with other couplings. On combining the results from both hadronic and leptonic modes and errors with luminosity uncertainty at 1% we find that the error sensitivity of $|V_{tb}| \Delta f_1^L \sim 10^{-3}$ becomes comparable to that observed in the bin analysis. The sensitivity is further reduced to 10^{-2} for luminosity uncertainty greater than 5%. However, sensitivity of all other couplings are unchanged at $\sim 10^{-4}$.

4.2 Comparison and Analysis

We compare our results with those quoted in the joint report *TOPLHCNOTE* [22], based on the recent experimental data at $\sqrt{s} = 7 \text{ TeV}$ and integrated luminosity of 35 pb^{-1} to 2.2 fb^{-1} . They found the sensitivity of the $Re(f_2^R) = 0.10 \pm 0.06(stat.) +_{-0.08}^{+0.07}(syst.)$. Performing the analysis for the LHeC with $E_p = 7 \text{ TeV}$, $E_e = 60 \text{ GeV}$ and integrated luminosity of 100 fb^{-1} , we find the upper limit on anomalous coupling $|f_2^R| \simeq 0.011$ and 0.01 for the hadronic and leptonic modes, respectively.

Alternatively, one constrains the C_{tW}/Λ^2 , a coefficient of dimension six operator $O_{tW} = (\bar{q} \sigma^{\mu\nu} \tau^I t) \tilde{\phi} W_{\mu\nu}^I$ that contribute to the Wtb anomalous coupling. By

translating the upper bound on the f_2^R on the upper limit of the coefficient corresponding to the dimension six operator, we find $|C_{tW}/\Lambda^2| \leq 0.13 \text{ TeV}^{-2}$.

However, the limit from low energy electroweak precision data on the above operator is much stronger $\sim |C_{tW}/\Lambda^2| \leq 0.4 \pm 1.2 \text{ TeV}^{-2}$ [17] than the present LHC bound and till date it provides the benchmark upper limit on the coefficient for this operator. Electroweak precision data also constrains the other coefficient $C_{bW}/\Lambda^2 \leq 11 \pm 13$ associated with dimension six operator $O_{bW} = (\bar{q} \sigma^{\mu\nu} \tau^I b) \phi W_{\mu\nu}^I$. Translating the upper bound from the coefficient f_2^L , we find that the proposed LHeC will improve the bound to a level of 10^{-2} as evident from equation (22).

Recently, a detailed study on the top anomalous couplings for LHC at 14 TeV with 10 fb^{-1} data [24] is done. They have computed the effect of the anomalous couplings at both production and decay vertices into the full t channel matrix element of the single top quark production and illustrated that one sigma contours on the plane of the anomalous couplings lie within order of magnitude $\sim 10^{-1}$. Therefore, the accuracy with which these couplings are measured at LHC can then be improved upon in the proposed LHeC as shown in Figures 7, 8, 9, 10 from the bin analysis.

At present the stringent upper bound on the magnitude of the anomalous couplings exist from the low energy B physics experiments as mentioned in the introduction and given in references [5–9]. On comparing with these limits we find that the LHeC might be able to measure these anomalous couplings at the same level of accuracy or even can do better with a high luminosity facility having luminosity uncertainty $\leq 1\text{-}2\%$.

The single top quark production process at ILC is realized through $e^+ + e^- \rightarrow t + \bar{b} + e^- + \bar{\nu}_e$ which is sub-dominant in comparison to the top pair production process $e^+ + e^- \rightarrow t + \bar{t}$. Therefore, the sensitivity analysis of Wtb anomalous couplings at ILC have been performed in the top pair production processes followed by their decay in hadronic, semi-leptonic and leptonic decay modes [54–56]. Boos *et. al* [55] have simulated the observables forward-backward asymmetry, spin-spin asymmetry of the top/anti-top decay products and the asymmetry of the lepton energy spectrum for their analysis of Wtb couplings and found that 2σ exclusion contours predict that no distinction can be made with SM if $f_2^L \in [-0.025, 0]$ and $f_2^R \in [-0.20, 0.20]$. Another, study by Batra and Tait shows the sensitivity of the anomalous couplings are of the order of $\sim 3\%$ with 100 fb^{-1} data [56]. Errors in the measurement at ILC can however, drastically reduced by improving the top/ anti-top reconstruction tools like b -tagging efficiency, the vertex charge determination and

the top identification, though ILC is better suited top explore the sensitivity of the dimension six operators associated with flavour conserving and flavor changing neutral currents [57, 58].

Our analysis shows that we can probe the Wtb vertex at the LHeC to a very high accuracy and can obtain much more stringent upper limits on anomalous couplings, in comparison to existing limits from the LHC, electroweak physics and B meson decays. The arXiv version of this study has been discussed in the High Energy Particle Physics Workshop 2015 [37], LHeC Workshop 2015 [59] and in the DIS 2015 workshop [60]. We hope that our report will be useful in studying the physics potential of the LHeC project.

Acknowledgements SD, AG and MK would like to acknowledge the partial support from DST, India under grant SR/S2/HEP-12/2006. AG would like to acknowledge CSIR (ES) award for the partial financial support.

References

1. G. L. Kane, G. A. Ladinsky and C. P. Yuan, Phys. Rev. D **45**, 124 (1992).
2. J. A. Aguilar-Saavedra, Nucl. Phys. B **812**, 181 (2009).
3. J. A. Aguilar-Saavedra, Nucl. Phys. B **821**, 215 (2009).
4. H. S. Do, S. Groote, J. G. Korner and M. C. Mauser, Phys. Rev. D **67**, 091501 (2003).
5. F. Larios, M. A. Perez and C. P. Yuan, Phys. Lett. B **457**, 334 (1999).
6. G. Burdman, M. C. Gonzalez-Garcia and S. F. Novaes, Phys. Rev. D **61**, 114016 (2000).
7. E. Barberio *et al.* [Heavy Flavor Averaging Group (HFAG) Collaboration], arXiv:0704.3575 [hep-ex].
8. B. Grzadkowski and M. Misiak, Phys. Rev. D **78**, 077501 (2008) [Erratum-ibid. D **84**, 059903 (2011)].
9. J. Drobnak, S. Fajfer and J. F. Kamenik, Nucl. Phys. B **855**, 82 (2012).
10. V. M. Abazov *et al.* [D0 Collaboration], Phys. Rev. Lett. **100** (2008) 062004.
11. V. M. Abazov *et al.* [D0 Collaboration], Phys. Rev. Lett. **103**, 092001 (2009).
12. CDF/PUB/TOP/PUBLIC/10793
13. S. Chatrchyan *et al.* [CMS Collaboration], JHEP **1212**, 035 (2012).
14. G. Aad *et al.* [ATLAS Collaboration], Phys. Lett. B **717**, 330 (2012).
15. V. M. Abazov *et al.* [D0 Collaboration], Phys. Lett. B **713**, 165 (2012).
16. B. Sahin and A. A. Billur, Phys. Rev. D **86**, 074026 (2012).

17. C. Zhang, N. Greiner and S. Willenbrock, *Phys. Rev. D* **86**, 014024 (2012).
18. N. Greiner, S. Willenbrock and C. Zhang, *Phys. Lett. B* **704**, 218 (2011).
19. J. Drobnak, S. Fajfer and J. F. Kamenik, *Phys. Rev. D* **82**, 114008 (2010).
20. J. A. Aguilar-Saavedra, J. Carvalho, N. F. Castro, F. Veloso and A. Onofre, *Eur. Phys. J. C* **50**, 519 (2007).
21. ATLAS-CONF-2011-037.
22. ATLAS-CONF-2013-033; CMS PAS TOP-12-025.
23. J. A. Aguilar-Saavedra, N. F. Castro and A. Onofre, *Phys. Rev. D* **83**, 117301 (2011).
24. F. Bach and T. Ohl, *Phys. Rev. D* **86**, 114026 (2012).
25. K. Ciekiewicz and K. Kolodziej, *Acta Phys. Polon. B* **34**, 5497 (2003).
26. B. Grzadkowski and Z. Hioki, *Phys. Lett. B* **557**, 55 (2003).
27. S. D. Rindani, *Pramana* **54**, 791 (2000).
28. Alwall:2011uj K. Kolodziej, *Phys. Lett. B* **584**, 89 (2004).
29. S. Atag, O. Cakir and B. Dilec, *Phys. Lett. B* **522**, 76 (2001).
30. J. L. Abelleira Fernandez *et al.* [LHeC Study Group Collaboration], *J. Phys. G* **39**, 075001 (2012).
31. J. L. Abelleira Fernandez, C. Adolphsen, P. Adzic, A. N. Akay, H. Aksakal, J. L. Albacete, B. Allanach and S. Alekhin *et al.*, arXiv:1211.4831 [hep-ex].
32. O. Bruening and M. Klein, *Mod. Phys. Lett. A*, Vol. 28, No. **16**, 1330011 (2013).
33. A. Senol, *Nucl. Phys. B* **873**, 293 (2013).
34. S. S. Biswal, R. M. Godbole, B. Mellado and S. Raychaudhuri, *Phys. Rev. Lett.* **109**, 261801 (2012).
35. T. Han and B. Mellado, *Phys. Rev. D* **82**, 016009 (2010).
36. J. L. Abelleira Fernandez *et al.* [LHeC Study Group Collaboration], arXiv:1211.5102 [hep-ex].
37. M. Kumar, arXiv:1506.03999 [hep-ph];
38. A. Andreazza, M. Anselmino, P. Azzi, W. Baldini, R. Barbieri, F. Bedeschi, E. Bertuzzo and C. Biino *et al.*, *Frascati Phys. Ser.* **60**, 1 (2015). S. Forte, A. Nisati, G. Passarino, R. Tenchini, C. M. C. Calame, M. Chiesa, M. Cobal and G. Corcella *et al.*, arXiv:1505.01279 [hep-ph];
39. I. A. Sarmiento-Alvarado, A. O. Bouzas and F. Larios, *J. Phys. G* **42**, no. 8, 085001 (2015);
40. K. Agashe *et al.* [Top Quark Working Group Collaboration], arXiv:1311.2028 [hep-ph]; [41]
41. A. O. Bouzas and F. Larios, *Phys. Rev. D* **88**, no. 9, 094007 (2013).
42. S. Dutta, A. Goyal and M. Kumar, *Phys. Rev. D* **87**, 094016 (2013).
43. I. T. Cakir, A. Senol and A. T. Tasci, arXiv:1301.2617 [hep-ph].
44. I. T. Cakir, O. Cakir and S. Sultansoy, *Phys. Lett. B* **685**, 170 (2010).
45. J. Alwall, M. Herquet, F. Maltoni, O. Mattelaer and T. Stelzer, *JHEP* **1106**, 128 (2011).
46. A. Alloul, J. D'Hondt, K. De Causmaecker, B. Fuks and M. R. de Trautenberg, *Eur. Phys. J. C* **73**, 2325 (2013).
47. S. Chatrchyan *et al.* [CMS Collaboration], *JHEP* **1310**, 167 (2013); CMS Collaboration [CMS Collaboration], CMS-PAS-TOP-14-017.
48. J. A. Aguilar-Saavedra, J. Carvalho, N. F. Castro, A. Onofre and F. Veloso, *Eur. Phys. J. C* **53**, 689 (2008).
49. S. Dutta, K. Hagiwara and Y. Matsumoto, *Phys. Rev. D* **78**, 115016 (2008); J. F. Gunion and J. Pliszka, *Phys. Lett. B* **444**, 136 (1998); J. F. Gunion, B. Grzadkowski and X. G. He, *Phys. Rev. Lett.* **77**, 5172 (1996) *Phys. Lett. B* **444**, 136 (1998).
50. O. Nachtmann and F. Nagel, *Eur. Phys. J. C* **40** (2005) 497; M. Diehl, O. Nachtmann and F. Nagel, *Eur. Phys. J. C* **27**, 375 (2003); M. Diehl and O. Nachtmann, *Eur. Phys. J. C* **1**, 177 (1998).
51. G. K. Fanourakis, D. Fassouliotis and S. E. Tzamarias, *Nucl. Instrum. Meth. A* **414**, 399 (1998).
52. P. Achard *et al.* [L3 Collaboration], *Phys. Lett. B* **597**, 119 (2004); P. Achard *et al.* [L3 Collaboration], *Phys. Lett. B* **586**, 151 (2004).
53. A. Heister *et al.* [ALEPH Collaboration], *Eur. Phys. J. C* **21**, 423 (2001); A. Heister *et al.* [ALEPH Collaboration], *Eur. Phys. J. C* **19**, 1 (2001); P. Abreu *et al.* [DELPHI Collaboration], *Phys. Lett. B* **423**, 194 (1998).
54. J. A. Aguilar-Saavedra and R. V. Herrero-Hahn, *Phys. Lett. B* **718**, 983 (2013); E. Devetak, arXiv:0810.4831 [hep-ex]; R. Frey, In *Morioka-Appi 1995, Physics and experiments with linear colliders* 144-178 [hep-ph/9606201].
55. E. Boos, M. Dubinin, M. Sachwitz and H. J. Schreiber, *Eur. Phys. J. C* **16**, 269 (2000).
56. P. Batra and T. M. P. Tait, *Phys. Rev. D* **74**, 054021 (2006).
57. H. Baer *et al.*, *The International Linear Collider Technical Design Report - Volume 2: Physics*, arXiv:1306.6352 [hep-ph].
58. M. S. Amjad *et al.*, arXiv:1505.06020 [hep-ex]; R. R  ntschi and M. Schulze, *JHEP* **1508**, 044 (2015); M. S. Amjad *et al.*, arXiv:1307.8102; J. A. Aguilar-Saavedra, M. C. N. Fiolhais and

-
- A. Onofre, JHEP **1207**, 180 (2012); M. C. N. Fiolhais, J. Phys. Conf. Ser. **447**, 012032 (2013); S. Groot, J. G. Korner, B. Melic and S. Prelovsek, arXiv:1209.0547 [hep-ph].
59. LHeC Workshop 2015 at CERN on 24 June 2015 and at Chavannes-de-Bogis on 25-26 June 2015.
60. DIS 2015 - XXIII. International Workshop on Deep-Inelastic Scattering and Related Subjects, 27 April-1 May, 2015 at Dallas, Texas, USA.